

# Measuring cell adhesion forces during the cell cycle by force spectroscopy

Gilles Weder<sup>a)</sup>

Swiss Centre for Electronics and Microtechnology, CSEM SA, Nanotechnology and Life Sciences, Jaquet-Droz 1, CH-2002 Neuchâtel, Switzerland and Department of Information Technology and Electrical Engineering, Laboratory of Biosensors and Bioelectronics, Institute for Biomedical Engineering, ETH Zurich, Gloriastrasse 35, CH-8092 Zurich, Switzerland

Janos Vörös

Department of Information Technology and Electrical Engineering, Laboratory of Biosensors and Bioelectronics, Institute for Biomedical Engineering, ETH Zurich, Gloriastrasse 35, CH-8092 Zurich, Switzerland

Marta Giazzon, Nadège Matthey, Harry Heinzemann, and Martha Liley

Swiss Centre for Electronics and Microtechnology, CSEM SA, Nanotechnology and Life Sciences, Jaquet-Droz 1, CH-2002 Neuchâtel, Switzerland

(Received 19 February 2009; accepted 29 April 2009; published 21 May 2009)

Force spectroscopy has been used to measure the adhesion of Saos-2 cells to a glass surface at different phases of the cell cycle. The cells were synchronized in three phases of the cell cycle:  $G_1$ ,  $S$ , and  $G_2M$ . Cells in these phases were compared with unsynchronized and native mitotic cells. Individual cells were attached to an atomic force microscope cantilever, brought into brief contact with the glass surface, and then pulled off again. The force-distance curves obtained allowed the work and maximum force of detachment as well as the number, amplitude, and position of discrete unbinding steps to be determined. A statistical analysis of the data showed that the number of binding proteins or protein complexes present at the cell surface and their binding properties remain similar throughout the cell cycle. This, despite the huge changes in cell morphology and adhesion that occur as the cells enter mitosis. These changes are rather associated with the changes in cytoskeletal organization, which can be quantified by force spectroscopy as changes in cell stiffness. © 2009 American Vacuum Society. [DOI: 10.1116/1.3139962]

## I. INTRODUCTION

For most adherent cells *in vitro*, dramatic changes in cell morphology take place during the cell cycle.<sup>1</sup> For most of the cell cycle, the cells are spread over the surface of the substrate. Then, at the beginning of mitosis, they round up and lose most of their contact to the substrate in preparation for cytokinesis. Mitotic rounding up is associated with changes in the cytoskeleton, plasma membrane, and cell volume, while adhesion of the cell to the substrate is greatly reduced.<sup>2</sup> However, the underlying mechanisms of these changes are poorly understood.

Adherent cells attach to their surroundings via focal adhesions. These large protein complexes consist of a variety of cytoskeletal and cytoskeletal-associated proteins providing the primary stabilizing force for the attachment of cultured cells as well as initiation sites for actin stress fibers.<sup>3,4</sup> There have been many studies of the role of individual adhesion proteins in the rounding up of mitotic cells.<sup>5</sup> These studies show that various phosphorylation events of cytoskeletal<sup>6</sup> and focal adhesion proteins<sup>7-12</sup> contribute to the premitotic disassembly of focal adhesions,<sup>13</sup> the deconstruction of the actin cytoskeleton of the interphase,<sup>14</sup> and the construction of a new mitotic cytoskeleton.<sup>15</sup> However, despite this dissociation and deconstruction, the mitotic cell remains attached to the substrate. There is direct contact be-

tween the plasma membrane and the substrate.<sup>16</sup> In addition, there are a number of retraction fibers, thin actin filaments, that anchor the cell to the substrate via focal adhesions. Thus some adhesive elements remain during mitosis.

Not only the cytoskeleton but also the plasma membrane is remodeled during mitosis. Rounding up of the cell involves a reduction in the total area of the plasma membrane, which has been recently found to take place via normal endocytosis of the plasma membrane and a reduction in the recycling of internalized membranes.<sup>17</sup>

In order to better understand the role of focal adhesions in the rounding up of cells during mitosis, we investigated the adhesion of osteosarcoma cells to a glass substrate at different phases of the cell cycle ( $G_1$ ,  $S$ , and  $G_2M$ ) using atomic force microscopy (AFM).<sup>18</sup> AFM was originally developed for high-resolution imaging but it has also become a powerful tool to manipulate biomolecules<sup>19,20</sup> or cells<sup>21,22</sup> and to investigate forces in the piconewton range.<sup>23,24</sup> In AFM force spectroscopy, the cantilever is moved toward a sample or a surface until it is in contact with it and then retracted while the interaction forces between the cantilever and surface are measured. Force spectroscopy allows direct measurement of the adhesive and mechanical properties of individual cells. These properties that are characteristic of the entire cell can then be correlated with molecular changes within the cell.<sup>25</sup>

In our investigations a single cell was attached to an AFM cantilever, brought briefly into contact with a glass substrate, and then pulled off the substrate<sup>26</sup> [Fig. 1(a)]. Measurement

<sup>a)</sup>Electronic mail: gilles.weder@csem.ch

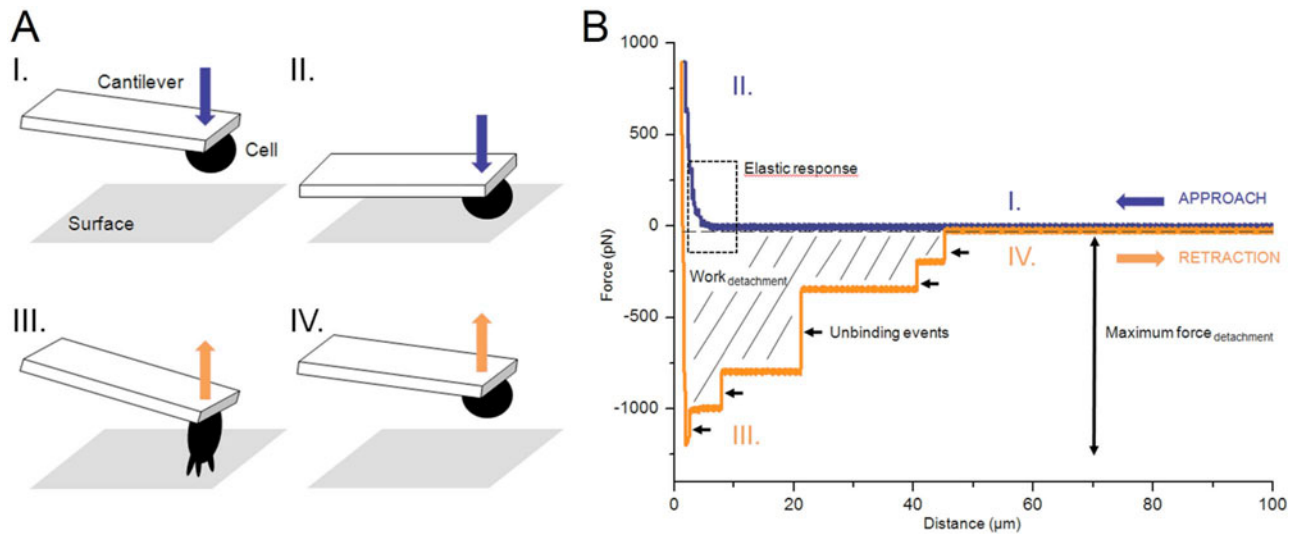


FIG. 1. (Color online) (a) Schematic of a single cell force spectroscopy measurement and (b) a force-distance curve acquired during approach (I and II) and retracting steps (III and IV). In the initial phase of the approach there is no contact between the cell and the surface (step I). Then the cell is pressed onto the surface until a preset maximal force is attained. During this phase the elastic response of the cell can be observed (step II). The position of the cantilever is held constant for a given contact time. Information on different mechanical parameters can be obtained from the retraction: the work of detachment, the number, amplitude, and position of the unbinding events corresponding to single proteins or protein complexes, and, finally, the maximal force needed to detach the cell from the surface (step III). In the last step, there is no physical contact between the cell and surface (step IV).

of the cantilever deflection during this process allowed the forces between the cell and surface to be quantified at each moment and represented in “force-distance curves” [Fig. 1(b)]. Several different mechanical parameters were extracted from these curves<sup>27</sup> including the maximum force of detachment, the displacement needed to completely remove the cell from the substrate, and the work of detachment. Not only global cellular parameters were studied: it was also possible to identify and analyze individual unbinding events, discrete steps in the force-distance curve that occur on the release of individual proteins or protein complexes from the surface.<sup>22</sup>

With this approach, the results obtained reflected the composition and organization of the plasma membrane, for example, concerning the presence, activity, and organization of adhesion proteins, as well as the stiffness of the cell cortex. However, the short contact time—1 s—between cell and substrate means that no information could be gained about how the cell responds to the surface on a longer time scale, thus excluding the effects of, for example, changes in protein expression.

The heterogeneity of the cell populations studied and the relatively wide variation observed in force-distance curves measured on one cell meant that a statistical analysis of the data was necessary to understand the significance of the many differences observed between the different cell cycle phases. The results of this analysis show that, despite the enormous changes undergone by the cell during mitosis, the initial cellular adhesion parameters remain broadly similar (throughout this article the word “similar” has been used in the sense of “alike but not identical,” not to be confused with “not statistically different”). In contrast, the stiffness of the

cell changes throughout the cell cycle and these changes are clearly reflected in the force-distance curves obtained.

## II. MATERIALS AND METHODS

### A. Cell culture

The human osteosarcoma cell line, Saos-2, was obtained from American Type Culture Collection (Manassas, VA) and was maintained in continuous culture in McCoy’s 5A medium supplemented with 10% heat-inactivated standardized fetal bovine serum (Biochrom AG, Germany), 50 units/ml of penicillin (Sigma, MO), 50  $\mu\text{g}/\text{ml}$  of streptomycin (Sigma, MO), and 1.5 mM of L-glutamine (Sigma, MO) at 37 °C in a humidified 5%  $\text{CO}_2$  atmosphere.

### B. Cell synchronization

Saos-2 cells were grown to about 60% confluency. Cell cycle arrest in the late  $G_1$  phase was induced using mimosine (Sigma, MO) synchronization. Mimosine was added to a final concentration of 0.4 mM and the cells were incubated for 48 h.

Cell cycle arrest in the late S phase was induced using thymidine (Sigma, MO) synchronization. Thymidine was added to a final concentration of 4 mM and the cells were incubated for 48 h. Cells were then washed twice in phosphate buffer solution (PBS) and incubated with regular medium for 8 h.

Cell cycle arrest in  $G_2M$  phase was induced using nocodazole (Sigma, MO) synchronization. Nocodazole-treated cells enter mitosis where they are blocked since they cannot form metaphase spindles. Nocodazole was added to a final

concentration of 0.6  $\mu\text{g}/\text{ml}$  and the cells were incubated for 48 h. Cells were then purified by gentle shaking and by pipetting them off the dish.

Native mitotic cells were also studied. These were obtained by agitating unsynchronized cultures of cells to detach mitotic cells from the polystyrene culture surface and then pipetting off the resulting cells.<sup>28,29</sup>

### C. Determination of cell cycle phase by flow cytometry

Cells were harvested by trypsinization, washed in PBS, collected by centrifugation, and fixed in cooled 70% ethanol for 1 h. Cells were collected by centrifugation once more and suspended in PBS containing 40  $\mu\text{g}/\text{ml}$  propidium iodide (Sigma, MO), 0.015% v/v Nonidet P40 substitute (Sigma, MO), and 100  $\mu\text{g}/\text{ml}$  RNase A (Sigma, MO). After at least 30 min incubation on ice, the DNA content was analyzed in a FACSAria cell sorter (Becton Dickinson, CA). For each cell population, 15 000 cells were analyzed and the synchronization experiments were repeated at least five times. Data acquisition was performed with the FACSDIVA software (Becton Dickinson, CA) and further analysis of the data was carried out with the WINMDI software (J. Trotter, Scripps Research Institute, CA). Cells in phase  $G_2$  cannot be distinguished from those in  $M$  since they have the same amount of DNA.

### D. Atomic force microscopy

We used a Nanowizard II atomic force microscope (JPK Instruments, Germany) mounted on an Axiovert 200 inverted optical microscope (Carl Zeiss, Germany). A CellHesion module (JPK Instruments, Germany) allowed vertical displacements of the force microscope cantilever of up to 100  $\mu\text{m}$  while a BioCell incubation chamber (JPK Instruments, Germany) maintained the sample at 37 °C. 500  $\mu\text{m}$  long silicon tipless cantilevers (Arrow TL1, Nanoworld, Switzerland) with a nominal spring constant of 0.03 N/m were used for all AFM measurements. Cantilevers were calibrated using the thermal fluctuation method in water with the SPM software (JPK Instruments, Germany) before each measurement.

AFM cantilevers were functionalized with concanavalin A using a protocol adapted from Wojcikiewicz *et al.*<sup>30</sup> Cantilevers were cleaned in an oxygen plasma (Harrick plasma, NY) for 5 min and then incubated overnight at 37 °C in a solution of 0.6 mg/ml biotinamidocaproyl-labeled bovine serum albumin (Sigma, MO) in 100 mM  $\text{NaHCO}_3$ , pH 8.6. The cantilevers were then rinsed twice in PBS and incubated in a solution of 0.6 mg/ml streptavidin (Sigma, MO) in PBS at pH 7.3 for 30 min. After two further rinses in PBS, they were finally incubated in a solution of 0.6 mg/ml biotin-labeled concanavalin A (Sigma, MO) in PBS for 60 min.

### E. Cell capture

Saos-2 cells were detached from the culture dishes by incubating with a solution of 2.5 g/l trypsin and 0.38 g/l of

ethylenediaminetetraacetic acid (EDTA) for 5 min.  $G_2M$  synchronized and native mitotic cells were already partially or completely detached from the culture dishes but were also exposed to trypsin under identical conditions. The cells were directly transferred to regular medium supplemented with 25 mM 4-(2-hydroxyethyl)-1-piperazineethanesulfonic acid (HEPES) maintained at 37 °C in a BioCell chamber. Using the AFM in force capture mode, the extremity of a concanavalin A-decorated cantilever was precisely positioned above one cell. An approach step brought the cell and cantilever into contact for 2 s. This was immediately followed by a retraction step to remove the cell from the surface. The cell was then left undisturbed on the cantilever for 15 min to ensure strong adhesion between the cell and cantilever.  $G_2M$  synchronized cells were most difficult to capture on the cantilever because of their higher stiffness.

### F. Force-distance curves

Force-distance curves were acquired with an approaching and retracting speed of 5  $\mu\text{m}/\text{s}$  using the maximum  $z$  range of 100  $\mu\text{m}$ . The cell was approached toward the surface until a repulsive force of 900 pN was reached. It was left in contact with the surface for 1 s before the retract step was started. There was a pause of 60 s at the maximal retract distance between each measurement.

For each cell the first and last force-distance curves were compared to ensure that there were no gross differences due to cell damage. To ensure that the cell-surface contact areas were similar for all measurements, the largest and smallest cells of each population—in total no more than 20% of the population—were excluded from measurements. All the measurements were carried out at 37 °C in McCoy's 5A medium supplemented with 1.5 mM L-glutamine and 25 mM HEPES buffer on a glass coverslip (Milian, Switzerland).

### G. Data processing and statistical analysis

The force-distance curves were analyzed to obtain the mechanical parameters related to cell detachment from the surface (Fig. 1) The parameters analyzed in this study were the work required to detach the cell from the substrate, the maximum force of detachment, and the number, position, and amplitude of the discrete detachment steps observed along the retraction curve. Data analysis was carried out using ORIGIN 7.5 (OriginLab, MA). For each cell population, ten force-distance curves were obtained from ten different cells, giving 100 measurements. However, not all these data are independent: results from any one cell are dependent, while data compared between cells are independent. For this reason, except where otherwise noted, the median value of each parameter was determined separately for each cell. The mean of these median values was then taken as characteristic for each condition. The data obtained were analyzed with the statistical analysis and data analysis software S-PLUS 8.0 (Insightful, Switzerland).

## H. AFM measurements of cell elasticity

Cell elasticity measurements were performed with the same AFM and cantilevers as described in Sec. II D but without tip functionalization. Cells were not trypsinized but were left attached to the polystyrene culture surface. Arrow TL1 tipless cantilevers were modified (Novascan, IA) by gluing glass spheres (radius=5  $\mu\text{m}$ , Novascan, IA) to the end of each cantilever to give well-defined indenters.<sup>31</sup>

Force-distance curves were acquired with a low approach speed of 2.5  $\mu\text{m/s}$  to minimize hydrodynamic effects. A maximum applied force of 200 pN resulted in a maximal indentation of 300 nm for the softest samples. The approach parts of the force indentation curves were fitted using a Hertzian model based on the assumption that the indenter was nondeformable. The fit was carried out using the software provided with the atomic force microscope (JPK Instruments, Germany) to estimate Young's modulus.

Mean values for Young's modulus were obtained by recording five force-distance curves on each of 20 different cells for both  $G_2M$  synchronized and unsynchronized cells. There was a pause of 60 s between each measurement. Measurements were performed only on thicker regions of the cell to avoid any influence of the underlying stiff glass substrate.

## III. RESULTS AND DISCUSSION

### A. Cell cycle synchronization in three phases

Saos-2 cells were synchronized in three phases of the cell cycle,  $G_1$ ,  $S$ , and  $G_2M$ . Unsynchronized cell populations showed the expected distribution of 56% of cells in the  $G_1$  phase, 21% in the  $S$  phase, and 23% in the  $G_2M$  phase. Good synchronization was obtained in both the  $G_1$  phase with 78% of cells in  $G_1$  and in the  $G_2M$  phase with 80% of cells in  $G_2M$ .  $S$  phase synchronization was limited to 62% due to differences in resumption of the cell cycle for individual cells after release from the thymidine synchronization. We were unable to find a more specific synchronizing agent to synchronize the cells in the intermediate  $S$  phase of DNA replication.

When studying synchronized cells, it is important to be aware that the synchronizing agent may affect several properties of the cell; nocodazole, for example, inhibits with the polymerization of the microtubules. In order to exclude the possibility that any differences observed between  $G_2M$  cells and unsynchronized cells were an unexpected artifact due to the use of nocodazole, native mitotic cells were also investigated. Native mitotic cells were obtained from unsynchronized cell cultures and were separated from cells in other phases of the cell cycle, thanks to their reduced adhesion to the culture surface. Gentle agitation of the medium or culture support resulted in their release from the surface into the culture medium while other cells remained firmly attached.

### B. Presence of adhesion-protein complexes throughout the cell cycle

First experiments carried out with the Saos-2 cells were used to select the experimental parameters for the adhesion

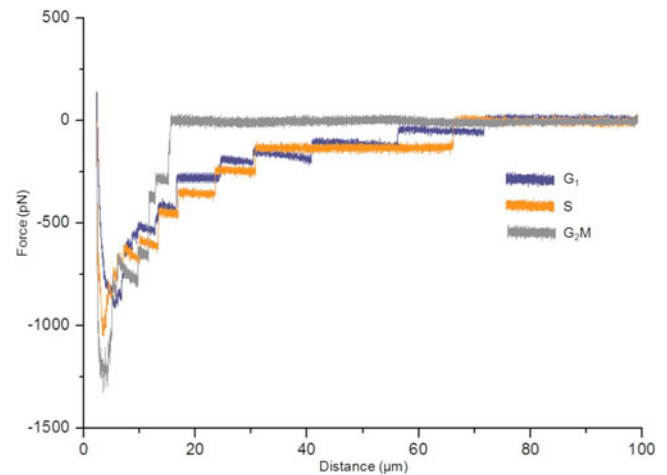


Fig. 2. (Color online) Typical force-distance curves showing the detachment of  $G_1$ ,  $S$ , and  $G_2M$  synchronized human osteoblasts from a glass surface (contact for 1 s with an applied force of 900 pN). The steplike features in the curves correspond to the release of adhesion proteins from the glass and can be observed in all three phases of the cell cycle.

measurements. An applied force of 900 pN was chosen to avoid the cell damage that can occur at higher forces, while a contact time of 1 s was selected to avoid very strong cell-surface interactions that may result either in cell rupture or in a failure to detach the cell from the surface even at a retraction distance of 100  $\mu\text{m}$ .

Using these experimental parameters, the typical force-distance curves obtained for each of the synchronized cell populations are shown in Fig. 2. Qualitatively, the curves look similar, with discrete unbinding events indicating the presence of adhesion-protein complexes at the cell membrane in each phase of the cell cycle. A statistical analysis of these events was carried out, comparing the number of events per curve, the amplitude of the events, and the position of the events along the retraction curve for the three synchronized cell populations and for a population of unsynchronized cells.

Histograms showing the number of unbinding events are shown in Fig. 3. In all cell populations, there were between 4 and 23 unbinding events per curve, reflecting the number of adhesion-protein complexes that bound to the surface. Comparing the mean numbers of unbinding events for the different populations (Table I) we see that in interphase ( $G_1$  and  $S$ ) the values obtained are 8.9 and 12, while in the two  $M$  phase populations ( $G_2M$  and native mitotic) the means are 11.3 and 10.9. For the unsynchronized cells, which we expect to be approximately 80% in interphase (since it is made up of 56%  $G_1$  and 21%  $S$ ), we obtain 12.6. The numbers of unbinding events in interphase and metaphase are broadly similar: we do not observe a large decrease in unbinding events that might be associated with a loss of adhesion in the  $M$  phase.

### C. Position of the unbinding events

The position (distance from the surface) of the unbinding events in the force-distance curves was also analyzed (Table II). Clear differences were observed between the  $G_2M$  phase

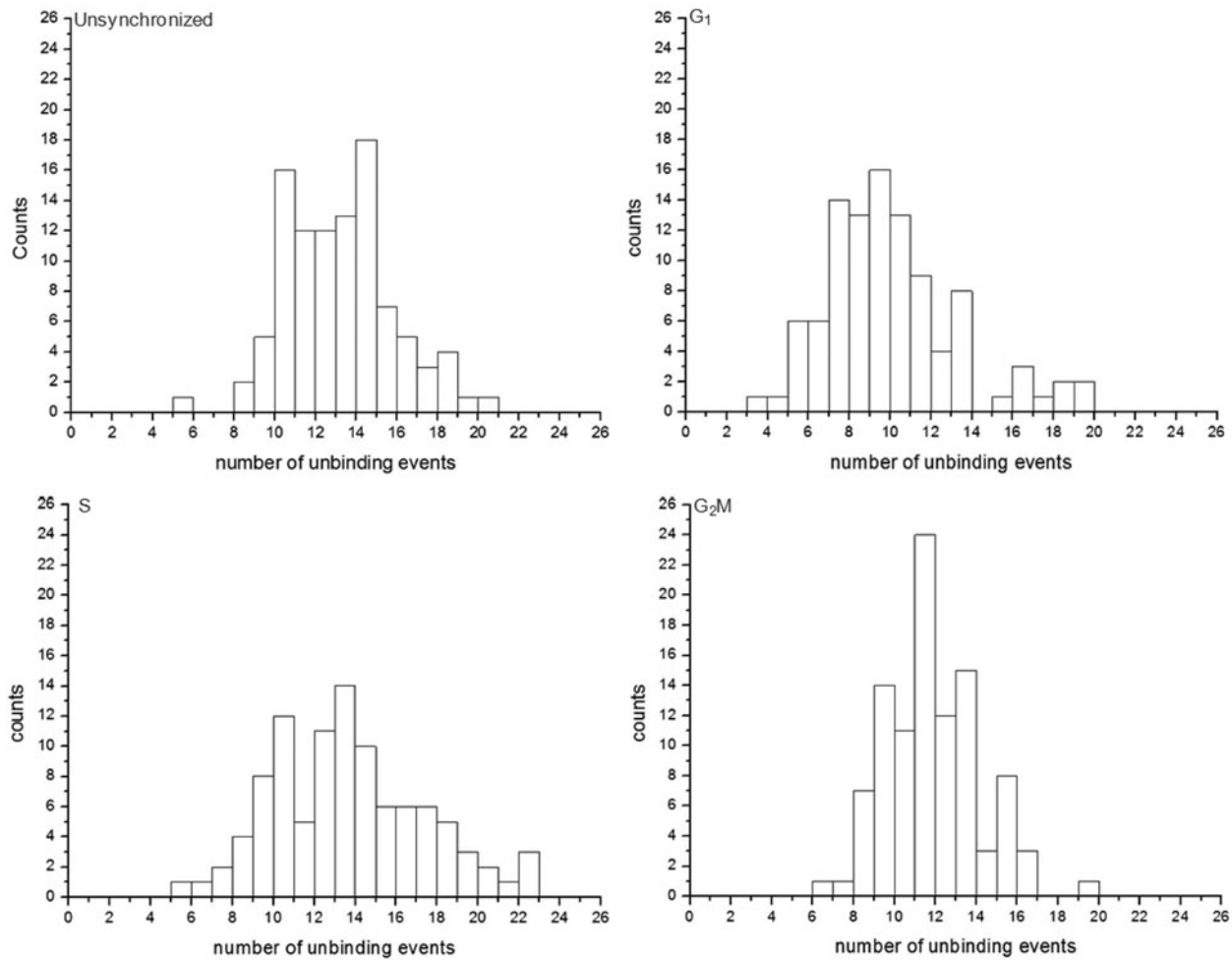


FIG. 3. Histograms showing the number of unbinding events of human osteoblasts on a glass surface after an applied force of 900 pN for 1 s. The number of unbinding events was measured for unsynchronized cells and synchronized cells in  $G_1$ ,  $S$ , and  $G_2M$  phases. Between 4 and 23 unbinding events were observed in each force-distance curve independently of the cell cycle phase.

and the other populations, while differences between unsynchronized and  $G_1$  and  $S$  phases were not significant. A statistical analysis of the number of events before and after 30  $\mu\text{m}$  displacement of the cantilever showed that the following:

- (1) For unsynchronized cells, 78% of unbinding events occur within the first 30  $\mu\text{m}$  and 22% in the remaining distance. Similar values were obtained for cells in  $G_1$  and  $S$ .
- (2) For cells in  $G_2M$ , 93% of unbinding events occur within the first 30  $\mu\text{m}$  and 7% in the remaining 70  $\mu\text{m}$  of travel.
- (3) For native mitotic cells, 95% of unbinding events occur within the first 30  $\mu\text{m}$  and 5% in the remaining 70  $\mu\text{m}$  of travel.

Clearly, cells in  $G_1$  and  $S$  can be stretched further before the cell is released from the surface than cells in  $G_2M$  or native mitotic cells.

#### D. Adhesion per protein complex in the different cell cycle phases

The amplitudes of the unbinding events are very similar in all the different conditions, with mean values between 84 and 108 pN (Table I). The size of these events suggests that they correspond to the rupture or release of either individual proteins or small protein complexes from the glass surface. This assumption is the basis of almost all single cell adhesion studies using force spectroscopy.

Comparing the values obtained for interphase ( $G_1$  and  $S$ ) with  $M$  phase ( $G_2M$  and native mitotic) we observe 86 and 84 pN, respectively, for the interphase populations and 108 and 96 pN for the  $M$  phase populations. In contrast, the unsynchronized population, which we expect to be approximately 80% in interphase, gives a value of 104 pN.

The similarity of the unbinding forces obtained for all phases of the cell cycle is perhaps surprising: there are numerous reports of the phosphorylation of individual proteins associated with the cytoskeleton and with focal adhesions,

TABLE I. Comparison of the number of unbinding events, the maximum force of detachment, the work of detachment, and the amplitude of the unbinding events for five conditions: unsynchronized cells,  $G_1$ ,  $S$ , and  $G_2M$  synchronized cells, and native mitotic cells (SE: standard error).

	Mean (median)	$\pm$ SE
(a) Number of unbinding events		
Unsynchronized	12.6	0.5
$G_1$ phase	8.9	0.4
$S$ phase	12	1
$G_2M$ phase	11.3	0.5
Native mitotic	10.9	0.8
(b) Amplitude of unbinding events		
Unsynchronized	104	17
$G_1$ phase	86	6
$S$ phase	84	13
$G_2M$ phase	108	5
Native mitotic	96	6
(c) Maximum force of detachment		
Unsynchronized	1.2	0.1
$G_1$ phase	0.88	0.03
$S$ phase	0.99	0.09
$G_2M$ phase	1.2	0.06
Native mitotic	1.2	0.06
(d) Work of detachment		
Unsynchronized	$1.9 \times 10^{-14}$	$0.2 \times 10^{-14}$
$G_1$ phase	$1.4 \times 10^{-14}$	$0.2 \times 10^{-14}$
$S$ phase	$1.7 \times 10^{-14}$	$0.2 \times 10^{-14}$
$G_2M$ phase	$1.1 \times 10^{-14}$	$0.1 \times 10^{-14}$
Native mitotic	$0.94 \times 10^{-14}$	$0.2 \times 10^{-14}$

which might lead one to expect differences (i.e., a reduction) in the binding ability of the proteins exposed at the cell membrane. This is not what we observed.

### E. Maximum force of detachment

The values obtained for the means of the maximum forces of detachment are similar for all phases of the cell cycle: the values, between 0.88 and 1.2 nN, are shown in Table I. Comparing interphase and  $M$  phase we obtain 0.88 and 0.99 nN for  $G_1$  and  $S$  populations and 1.2 nN for both  $G_2M$  and native mitotic cells. The unsynchronized population gives a value of 1.2 nN. We note that the maximum force of detachment is not strictly an independent parameter as it is related to the number of unbinding events and their amplitude. It is, however, not simply the product of the number of unbinding events and their amplitude due to contraction and/or relaxation of the cell during the measurement, particularly the first few microns of retraction.

The values obtained for the unsynchronized cell population are compatible with those obtained for each of the phases individually. The only significant differences are between the distributions of the  $G_1$  phase and mitotic cells.

One might expect the maximum forces of detachment to be the product of the number of unbinding events and their

TABLE II. Comparison of the distribution of the position of unbinding events between five conditions: unsynchronized cells,  $G_1$ ,  $S$ , and  $G_2M$  synchronized cells, and native mitotic cells.

	Position of unbinding events	
	$\leq 30 \mu\text{m}$ (%)	$> 30 \mu\text{m}$ (%)
Unsynchronized	78	22
$G_1$ phase	80	20
$S$ phase	79	21
$G_2M$ phase	93	7
Native mitotic	95	5

amplitude. This was, however, not the case due to contraction and/or relaxation of the cell during the measurement, particularly the first few microns.

### F. Work of detachment

The work of detachment—similarly to the maximum force of detachment—is not strictly an independent parameter as it is related to the amplitude and number of unbinding events and their position during retraction of the cantilever. The mean values for the work of detachment for the unsynchronized and synchronized cells are between  $1.9$  and  $0.94 \times 10^{-14}$  J (Table I). In interphase, the values obtained are  $1.4$  and  $1.7 \times 10^{-14}$  J for  $G_1$  and  $S$  populations. In  $M$  phase the values are  $1.1$  and  $0.94 \times 10^{-14}$  J for  $G_2M$  and native mitotic. For unsynchronized cells we obtained  $1.9 \times 10^{-14}$  J.

### G. Higher stiffness of mitotic cells

Our analysis of the positions of the unbinding events (Sec. II C) suggested that  $G_2M$  and native mitotic cells were stiffer than cells in the other phases. The increased stiffness of mitotic cells has been reported by other authors<sup>32,33</sup> and is associated with a reorganization of the cytoskeleton (Fig. 4). We verified this for our Saos-2 cells using force spectroscopy to obtain an estimate of Young's modulus of the cells. For these measurements, the cells were adherent on a glass surface and a round glass sphere attached to an AFM cantilever was brought into contact with them. Given the size of the glass sphere and the forces applied during the indentation process it was possible to calculate a value for Young's modulus. Mean values for the Young's modulus of individual  $G_2M$  synchronized cells and individual adherent unsynchronized cells are shown in Fig. 5. Typically, Young's moduli of the  $G_2M$  synchronized cells (mean value of 1.4 kPa) are higher than those of the unsynchronized cells (mean value of 0.4 kPa), confirming the increase in the cell stiffness in mitosis. The data obtained are within reported values for Young's modulus of living cells [between 0.1 and 10 kPa (Refs. 34 and 35)]. It is difficult to make close comparisons with literature values given the range of experimental parameters that influence the values obtained (e.g., geometry of the indenter, depth of indentation, speed of measurement). However, studies on osteosarcoma cell lines and on primary hu-

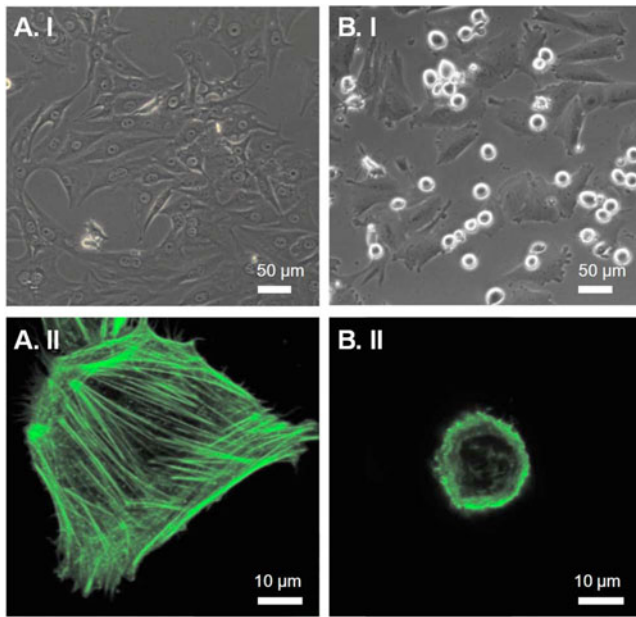


FIG. 4. (Color online) Comparison of (a) unsynchronized and (b)  $G_2M$  synchronized cells (b) by optical (i) and confocal microscopies (II) showing the actin fibers (labeled with AlexaFluor 488 Phalloidin). The cell rounding and reorganization of the cytoskeletal actin fibers observed in (b) are characteristic of cytokinesis.

man bone cells including osteoblasts give very similar Young's moduli: between 1 and 2 kPa for MG-63 cells,<sup>36</sup> from 0.7 to 2.6 kPa for primary human bone cells and MG-63,<sup>35</sup> and from 2.1 to 8.8 kPa for Saos-2 cells.<sup>37</sup>

## H. Discussion

We have used force spectroscopy to study the adhesion and mechanical properties of Saos-2 osteosarcoma cells at different phases in the cell cycle. Force spectroscopy is inherently a single cell technique: values for different mechanical properties are determined individually for each cell of each population studied. Single cell analyses allow us to study not only the average properties of a sample (an ensemble of cells) but also the variation and heterogeneity within the sample. While this gives access to qualitatively new information, it also comes with its disadvantages. In our case, the statistical analysis was made significantly more complicated: for each cell condition ten cells were selected for study—this relatively small number was chosen because of the lengthy preparation required for measurements on each individual cell—and ten force-distance measurements were carried out per cell. This method gave a data set that was a mix of dependent and independent results. In general, the analysis required that the data for each cell (dependent results) were analyzed first to obtain a value characteristic of that cell. The values for each cell in the sample were then analyzed as independent data points to give a value that was representative of the sample as a whole.

A significant limitation of this study is the use of trypsin to detach the cells from the culture surface before fixing them to the cantilever. Trypsinization clearly damages at

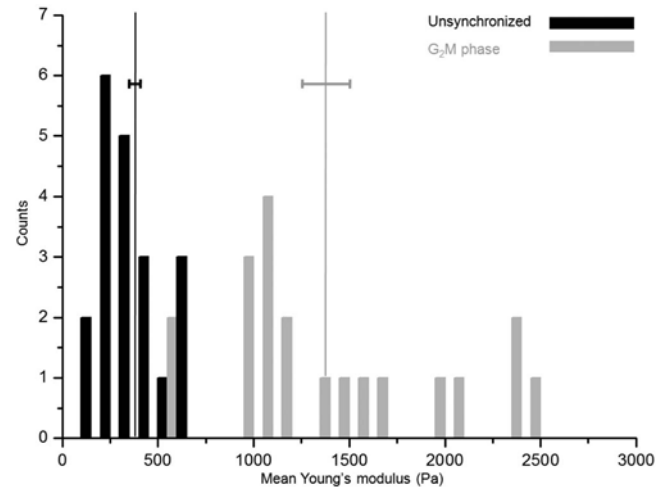


FIG. 5. Histogram showing the mean values of Young's modulus obtained for individual unsynchronized cells and cells synchronized in  $G_2M$  phase. Vertical lines indicate the mean of the means and the error bar is the standard error. No native mitotic cells were chosen for measurement in the unsynchronized cell population.

least some of the binding proteins exposed at the cell surface and so may well influence results in a study of these proteins. We have tried to minimize the effects observed by using a short, reproducible trypsinization on all samples and allowing the cells to recover for 30 min before measurement. Studies by other authors have shown that, at least in some cases, trypsinization leaves the binding functions of surface proteins largely intact.<sup>38,39,22</sup> Sodium dodecyl sulfate polyacrylamide gel electrophoresis (SDS-PAGE) analyses also showed no effect of the trypsinization on either  $\alpha 2$  integrin or  $\beta 1$  integrin.<sup>38</sup> Indeed, we saw no gross differences between trypsinized and untrypsinized native mitotic cells (data not shown). While trypsinization may limit our work to the observation of relatively large effects, we do not believe it has an influence on the conclusions of this study.

Finally, the short contact time between cell and surface during this study limits the analysis to a study of proteins and protein complexes that are already present at the cell membrane and to the gross mechanical properties of the cell. There is insufficient time for the cell to react significantly to the presence of the surface, for example, by changes in the cytoskeleton or in protein expression. A more complete study of cell-surface interactions requires much longer contact times between the cell and surface. However, in our hands, increased contact times between SaOs-2 cells and glass result in increased cell/surface adhesion and our attempts at force spectroscopy result either in rupture of the cell as cantilever and surface are separated or, alternatively, the cell does not rupture but does not release the surface either, remaining attached to both surface and cantilever even at separations of 100  $\mu\text{m}$ . To date, we have not found a suitable approach to measuring deadhesion curves for living Saos-2 cells at longer contact times.

#### IV. CONCLUSIONS

We have used single cell force spectroscopy to study the adhesive and mechanical properties of Saos-2 cells in culture. The study focused, in particular, on the changes in these properties between interphase, when cells are well spread and firmly attached to culture surface, and *M* phase, when the cells round up and are much more loosely attached to the surface. The differences in cell/surface attachment are striking: in *M* phase Saos-2 cells may be removed by shaking or tapping culture vessels while in interphase attempts to pull Saos-2 cells off the surface may result in cell rupture.

Because of the short time of contact between the cell and surface, our investigation is relevant to cell-surface properties and cell stiffness. The experiments described here show that binding proteins and/or protein complexes at the cell membrane remain similar both in number [Table I, (a)] and in their binding properties [amplitude of the unbinding event: Table I, (b)] during interphase and *M* phase. While some differences can be observed in the mean values obtained in the different phases, the differences are, in all cases, less than a factor of 1.5 and the extreme values are not associated with the  $G_2/M$  or native mitotic (*M*) phase. We do not observe a large reduction either in the number or in the amplitude of the unbinding events that might contribute to the loss of adhesion of *M* phase cells. This may be surprising given the numerous studies showing the phosphorylation of proteins associated with focal adhesions during mitosis.

A second clear conclusion can be drawn from the position of the unbinding events. As the cell was stretched during detachment from the surface, unbinding events took place at a smaller extension for the mitotic/ $G_2M$  cells than for cells in other phases. These cells cannot be stretched as far as before they are released from the surface. This is due to an increased stiffness of the cell caused by a reorganization of the cytoskeleton during mitosis as also observed by other researchers in the field.

The maximum force of detachment and the work of detachment were also studied for all the cells. These two parameters are not strictly independent as they are related to the number and amplitude of unbinding events and to their position. Here, again the differences observed between *M* phase and interphase were relatively small compared to the differences between cellular adhesion during the cell cycle.

We conclude, therefore, that the rounding up and greatly reduced adhesion of cells during *M* phase is not associated with large differences in the binding proteins in the cell membrane or in the adhesive properties of the cell on first contact. Instead, these effects may be associated with cytoskeletal changes and/or with changes in the interactions between surface proteins and other proteins either in the cell membrane or in the cytoplasm.

Finally, we conclude that single cell force spectroscopy is a useful tool in the study of cell mechanical and adhesive properties and their changes during the cell cycle. The quantitative information obtained is highly complementary to that determined using molecular biology approaches.

#### ACKNOWLEDGMENTS

The authors would like to thank Jérôme Maris-Polesel for valuable discussions. They are especially grateful to Jacqueline Moret and Jürg Schelldorfer for advice in the statistical analysis. This present work was funded by the Newbone project of the 6th European Framework program.

- <sup>1</sup>K. Porter, D. Prescott, and J. Frye, *J. Cell Biol.* **57**, 815 (1973).
- <sup>2</sup>M. Théry and M. Bornens, *HFSP J.* **2**, 65 (2008).
- <sup>3</sup>C. A. Otey, *J. Cell Biol.* **111**, 721 (1990).
- <sup>4</sup>M. A. Schwartz, M. D. Schaller, and M. H. Ginsberg, *Annu. Rev. Cell Dev. Biol.* **11**, 549 (1995).
- <sup>5</sup>E. N. Pugacheva, F. Roegiers, and E. A. Golemis, *Curr. Opin. Cell Biol.* **18**, 507 (2006).
- <sup>6</sup>V. M. Fowler and E. J. Adam, *J. Cell Biol.* **119**, 1559 (1992).
- <sup>7</sup>M. Curtis, S. N. Nikolopoulos, and C. E. Turner, *Biochem. J.* **363**, 233 (2002).
- <sup>8</sup>J. D. Hildebrand, M. D. Schaller, and J. T. Parsons, *Mol. Biol. Cell* **6**, 637 (1995).
- <sup>9</sup>A. Ma, A. Richardson, E. M. Schaefer, and J. T. Parsons, *Mol. Biol. Cell* **12**, 1 (2001).
- <sup>10</sup>R. Yamaguchi, Y. Mazaki, K. Hirota, S. Hashimoto, and H. Sabe, *Oncogene* **15**, 1753 (1997).
- <sup>11</sup>Y. Yamakita, G. Totsukawa, S. Yamashiro, D. Fry, X. Zhang, S. K. Hanks, and F. Matsumura, *J. Cell Biol.* **144**, 315 (1999).
- <sup>12</sup>T. Suzuki and K. Takahashi, *J. Cell. Physiol.* **197**, 297 (2003).
- <sup>13</sup>D. M. Clarke, M. C. Brown, D. P. LaLonde, and C. E. Turner, *J. Cell Biol.* **166**, 901 (2004).
- <sup>14</sup>X. Tong and P. M. Howley, *Proc. Natl. Acad. Sci. U.S.A.* **94**, 4412 (1997).
- <sup>15</sup>A. Bellissent-Waydelich, M. T. Vanier, C. Albiges-Rizo, and P. Simon-Assmann, *J. Histochem. Cytochem.* **47**, 1357 (1999).
- <sup>16</sup>M. Théry and M. Bornens, *Curr. Opin. Cell Biol.* **18**, 648 (2006).
- <sup>17</sup>P. Kunda, A. E. Pelling, T. Liu, and B. Baum, *Curr. Biol.* **18**, 91 (2008).
- <sup>18</sup>G. Binnig, C. F. Quate, and C. Gerber, *Phys. Rev. Lett.* **56**, 930 (1986).
- <sup>19</sup>H. Clausen-Schaumann, M. Seitz, R. Krautbauer, and H. E. Gaub, *Curr. Opin. Chem. Biol.* **4**, 524 (2000).
- <sup>20</sup>H. Janovjak, M. Kessler, D. Oesterhelt, H. Gaub, and D. J. Muller, *EMBO J.* **22**, 5220 (2003).
- <sup>21</sup>J. Helenius, C. P. Heisenberg, H. E. Gaub, and D. J. Muller, *J. Cell Sci.* **121**, 1785 (2008).
- <sup>22</sup>E. P. Wojcikiewicz, X. Zhang, A. Chen, and V. T. Moy, *J. Cell Sci.* **116**, 2531 (2003).
- <sup>23</sup>C. A. Lamontagne, C. M. Cuerrier, and M. Grandbois, *Eur. J. Phys.* **456**, 61 (2008).
- <sup>24</sup>T. Ludwig, R. Kirmse, K. Poole, and U. S. Schwarz, *Eur. J. Phys.* **456**, 29 (2008).
- <sup>25</sup>M. Benoit, D. Gabriel, G. Gerisch, and H. E. Gaub, *Nat. Cell Biol.* **2**, 313 (2000).
- <sup>26</sup>M. Benoit and H. E. Gaub, *Cells Tissues Organs* **172**, 174 (2002).
- <sup>27</sup>C. M. Franz, A. Taubenberger, P. H. Puech, and D. J. Muller, *Sci. STKE* **2007**, p15 (2007).
- <sup>28</sup>W. Krek and J. A. DeCaprio, *Methods Enzymol.* **254**, 114 (1995).
- <sup>29</sup>T. Terasima and L. J. Tolmach, *Nature (London)* **190**, 1210 (1961).
- <sup>30</sup>E. P. Wojcikiewicz, X. Zhang, and V. T. Moy, *Biol. Proced. Online* **6**, 1 (2004).
- <sup>31</sup>R. E. Mahaffy, S. Park, E. Gerde, J. Kas, and C. K. Shih, *Biophys. J.* **86**, 1777 (2004).
- <sup>32</sup>A. S. Maddox and K. Burrige, *J. Cell Biol.* **160**, 255 (2003).
- <sup>33</sup>R. Matzke, K. Jacobson, and M. Radmacher, *Nat. Cell Biol.* **3**, 607 (2001).
- <sup>34</sup>D. Docheva, C. Popov, W. Mutschler, and M. Schieker, *J. Cell. Mol. Med.* **11**, 21 (2007).
- <sup>35</sup>D. Docheva, D. Padula, C. Popov, W. Mutschler, H. Clausen-Schaumann, and M. Schieker, *J. Cell. Mol. Med.* **12**, 537 (2008).
- <sup>36</sup>D. Shin and K. Athanasiou, *J. Orthop. Res.* **17**, 880 (1999).
- <sup>37</sup>J. Domke, S. Dannöhl, W. J. Parak, O. Müller, W. K. Aicher, and M. Radmacher, *Colloids Surf., B* **19**, 367 (2000).
- <sup>38</sup>A. Taubenberger, D. A. Cisneros, J. Friedrichs, P. H. Puech, D. J. Muller, and C. M. Franz, *Mol. Biol. Cell* **18**, 1634 (2007).
- <sup>39</sup>X. Zhang, S. E. Craig, H. Kirby, M. J. Humphries, and V. T. Moy, *Biophys. J.* **87**, 3470 (2004).